Turkish Journal of Electrical Engineering and Computer Sciences

Volume 24 | Number 3 Article 47

1-1-2016

Source detection and propagation of equal frequency voltage flicker in nonradial power system

ABDOLMAJID DEJAMKHOOY

ALI DASTFAN

ALIREZA AHMADYFARD

Turkish Journal of Electrical Engineering & Computer Sciences

http://journals.tubitak.gov.tr/elektrik/

Research Article

Turk J Elec Eng & Comp Sci
(2016) 24: 1351 – 1370

doi:10.3906/elk-1311-162

Source detection and propagation of equal frequency voltage flicker in nonradial power system

Abdolmajid DEJAMKHOOY*, Ali DASTFAN, Alireza AHMADYFARD
Faculty of Electrical Engineering, Shahrood University of Technology, Shahrood, Iran

Received: 19.11.2013 • **Accepted/Published Online:** 06.03.2014 • **Final Version:** 23.03.2016

Abstract: Nowadays electric power quality problems such as flicker (voltage fluctuation) are major concerns of electric companies and industrial consumers. Identification of flicker sources is an important stage in the flicker reduction process. Flicker source can be modeled as a nonlinear load whose admittance is intermittent and time-variant. In the steady state, fluctuation of voltage amplitude is a function of the impedance of flicker sources. In this paper, after calculating the gradient of voltage amplitudes and constructing a Jacobian matrix, criteria for flicker source detection are proposed. Therefore, by measuring voltage and current of each load in the power system, the contaminative loads are identified. In the next step, flicker propagation throughout the power system is investigated. For identifying the dominant flicker source, an algorithm based on a directed graph method is proposed. For different operation modes of flicker sources, the effects of their locations on dominating are analytically interpreted. The proposed methods are tested in a typical nonradial power system in which several flicker sources have been operated. The flicker sources are operated with equal fluctuation frequency and different operation modes. Simulation results show a good performance for the single point proposed method in flicker source detection. These results confirm that the proposed algorithm can identify dominant flicker source as expected for our theory.

Key words: Power quality, flicker, flicker power, Jacobian matrix, directed graph, adjacency matrix, enhanced phased-locked loop

1. Introduction

Voltage fluctuation is one of the power quality problems that has concerned both the operators and customers of power networks. These fluctuations cause variation of light intensity that is perceived by the human eye. This annoying and undesirable phenomenon is called flicker. The frequency range of voltage flicker is approximately between 0.1 and 35 Hz. The maximum fluctuation of voltage amplitude causing flicker is 0.1 of nominal voltage amplitude [1]. Loads with several power demands or intermittent power and current are main sources of flicker. Studies have demonstrated that wind power plants lead to fluctuation of network voltage [2]. In addition, loads that provide interharmonics may be flicker sources [1].

The most commonly used method for flicker measurement is the IEC proposed flicker meter [3]. Using the IEC standard flicker meter, short-time flicker level (p_{st}) and long-time flicker level (p_{lt}) can be measured [3]. The flicker meter was recently improved in [4]. These well-known parameters cannot tell us if a load is a flicker source or not. In a radial network, with calculating flicker flow direction, the position of flicker source relative to monitoring point is determined. For this aim, flicker power in [5] and V-I slope in [6] were used. The most

*Correspondence: majiddejam@shahroodut.ac.ir

significant drawback of these methods is that location of flicker sources cannot be determined clearly. These methods are only applied for radial networks. A new flicker index based on wavelet transform for nonstationary disturbances was introduced in [7]. By considering fluctuated voltage as a signal with interharmonics, a method was proposed in [8]. This method was based on interharmonics load flow. If frequency of flicker sources is similar, this method cannot detect flicker sources in a power system. Identification of flicker source in a distribution system using a multilevel perceptron neural network was presented in [9]. The authors utilized a radial single-side supplied power system for verifying their method. They assumed that only one flicker source was connected to the network. A power system with several flicker sources (especially if their fluctuation frequencies were equal) was not considered in the paper. In [10], the current of flicker sources that were supplied by a busbar was measured and the effect of each load was separated. However, in this work, a power system in which flicker sources had been distributed throughout the network was not investigated. The authors did not regard the similarity or dissimilarity of the flicker source frequencies. A method was proposed in [11] for identifying the location of the flicker source by minimizing measurements and estimating instantaneous voltage of buses. In [11] only a flicker source was assumed to be operating in the network and a multiflicker source situation was not investigated. Recently a mathematical approach to describe flicker propagation from downstream to upstream was presented in [12]. The authors focused on flicker that resulted from a wind farm. They employed a reactive power concept for their resolution. A power system with several wind farms, where their flicker frequency may be equal or dissimilar, was not considered. Significant influence of network impedance on the parameters that describe flicker severity was indicated in [13]. This result confirms our intention to undertake an analytical effort for detecting the locations of the flicker sources.

Detection of coupling points of flicker sources in power systems is necessary and important to convince industrial customers for applying enhancement procedures or penalty payments. If fluctuation frequencies of flicker sources are not equal, frequency difference can be used as a character to identify flicker sources. For equal fluctuation frequency of flicker sources, detection of coupling points of these sources is not an easy task. Therefore, regarding the amplitude modulation model of voltage fluctuation, the phase angle of the envelope signal becomes important. In other words, coherent or asynchronous operation of flicker sources, which is called operation modes, should be essentially attended to.

In this paper first an analytical theory for detecting loads that cause flicker is proposed. This single point method needs the instantaneous voltage and current of each load. Since impedance variation of flicker sources causes fluctuation of amplitude of voltage and current, voltage and current gradients are calculated. The impedances of the contaminative loads are assumed as independent variables. After constructing the corresponding Jacobian matrix, the sign of flicker power for all possible conditions of the contaminative loads is analyzed. Then a criterion based on the sign of the flicker power is provided to detect flicker sources.

In the next stage, a new algorithm based on a special defined directed graph for describing flicker propagation through the network is proposed. This algorithm can identify the dominant flicker source. Instantaneous voltage of system buses and current of transmission lines are utilized in this method. By assuming equal power demand for the contaminative loads as flicker sources, two main factors affect the dominating of flicker source: location of flicker sources at the power system and their operation modes. Finally, reasons for dominating the flicker source are analyzed and criteria for identifying the dominant flicker source are defined.

For evaluating the proposed methods, some simulations are conducted. A typical six-bus nonradial power system, in which several flicker sources are simultaneously operated, is studied. Some scenarios are suggested and simulated. In different scenarios the number, power demand, coupling points, and operation modes of the

flicker sources are changed, but in each simulation, fluctuation frequency of the flicker sources is assumed to be equal. Both the current and the voltage amplitude envelopes are extracted by enhanced phased-locked loop (EPLL), which is an adaptive nonlinear filter.

The rest of the paper is organized as follow. In the next section flicker modeling, envelope extraction of fluctuated voltage, and flicker power are explained briefly. The proposed single point method for detecting the flicker sources and the directed graph-based proposed algorithm for identifying the dominant flicker source in the power system are presented respectively in Sections 3 and 4. In Section 5 simulation results are given and discussed. Finally, in Section 6, conclusions are drawn.

2. Flicker modeling

2.1. Mathematical description of the flicker phenomenon

Amplitude modulation is adopted for modeling of voltage flicker. In this model one or several sinusoidal components as flicker tones are modulated in voltage amplitude [1]. In general the voltage flicker is represented as follows:

$$V\left(t\right)=V_c\left[1+\sum_{i=1}^{M}V_i\cos\left(\omega_i t+\theta_i\right)\right]\cos\left(\omega_c t+\theta_c\right), \tag{1}$$

where V_c is the nominal amplitude of the network voltage, ω_c is the supply angular frequency, and θ_c is the supply phase angle. For each i, $V_i\cos\left(\omega_i t+\theta_i\right)$ is a flicker tone where V_i is the amplitude, ω_i is the angular frequency, and θ_i is the phase angle of the ith flicker tone. When flicker sources fluctuate with the same frequency, as discussed in this paper, $M = 1$. Thus, the fluctuated voltage can be rewritten as follows:

$$V\left(t\right)=V_c\left[1+V cos\left(\omega t+\theta\right)\right]cos?(\omega_c t+\theta_c). \tag{2}$$

2.2. Envelope extracting using EPLL

Traditionally the phase-locked loop (PLL) has been employed to trace the phase of signal and has been applied widely in communication systems, servo machines, and speed control of synchronous motors [14]. A typical PLL consists of three distinct main parts: a phase detector (PD) that is a signal multiplier, loop filter (LF) that consists of a low-pass filter, and a voltage-controlled oscillator (VCO), which is a frequency-modulated oscillator [14].

A PLL that was enhanced for envelope extracting was proposed in [15], called the EPLL. A structural block diagram of the EPLL is shown in Figure 1. K, K_p, and K_i are known as EPLL parameters. Response time and tracking accuracy are two major criteria in EPLL performance that are controlled and tuned by means of EPLL parameters.

Error signal is defined as $e\left(t\right)=u\left(t\right)-y(t)$ where $u\left(t\right)$ is the input signal of the EPLL, and $y(t)$ is the fundamental component of input signal as demonstrated in Figure 1. The differential equations governing the EPLL are derived as follows [15]:

$$\begin{cases} \dot{A}(t)=K\,e(t)\ sin?(\varphi(t)) \\ \dot{\omega}\left(t\right)=K_i\,e\left(t\right)\ cos?(\varphi\left(t\right)) \\ \dot{\varphi}\left(t\right)=\omega\left(t\right)+\frac{K_p}{K_i}\dot{\omega}(t) \end{cases}, \tag{3}$$

where $A(t)$ is amplitude, $\omega(t)$ is angular frequency, and $\varphi(t)$ is the phase signal of the input signal of EPLL.

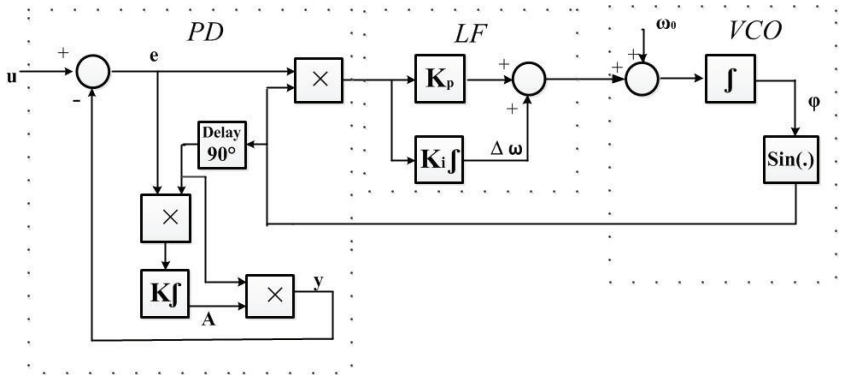

Figure 1. EPLL block diagram [15].

In this paper, the purpose of the EPLL application is envelope extraction of the instantaneous voltage. Since flicker sources are assumed to have the same frequency, the envelope signal is a sinusoidal component with flicker frequency. In other words, all flicker sources produce the same frequency tone. Exploiting the EPLL to voltage signal, the envelope of this signal can be extracted as follows:

$$m_V(t) = V cos(\omega t + \theta). \tag{4}$$

Regarding the flicker model described previously, the waveform for a voltage flicker signal with a flicker tone, 8% nominal voltage amplitude, and respectively 9 Hz is shown in Figure 2. The actual and extracted envelope of the fluctuated voltage is shown in Figure 3.

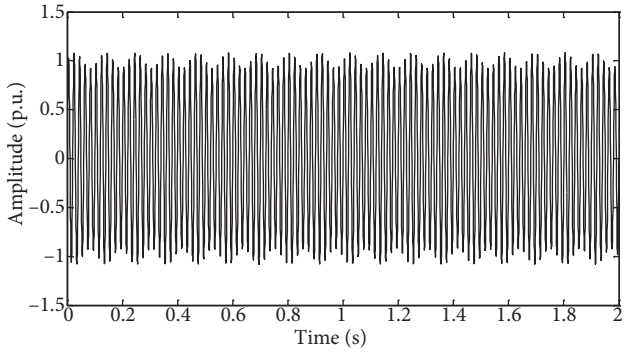

Figure 2. Fluctuated voltage with a flicker tone.

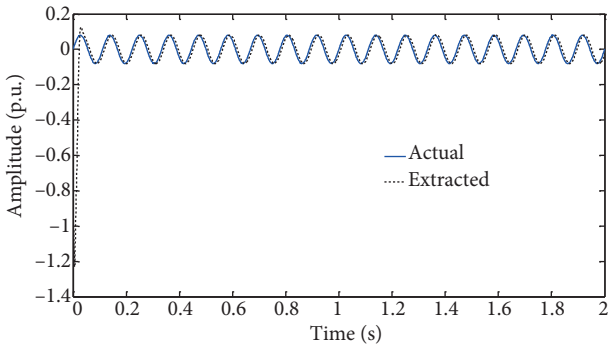

Figure 3. Envelope of fluctuated voltage.

2.3. Flicker power

Although flicker is defined as fluctuation of voltage signal, this phenomenon causes fluctuation in the current signal, too. In [5] flicker power as a new power quantity was proposed to describe flicker flow. The flicker power sign gives information about the direction of the flicker source. By multiplying the envelope signal of the voltage and current waveforms, instantaneous flicker power is achieved as follows:

$$fp\,(t) = m_v\,(t)\,.\,m_i\,(t)\,, \tag{5}$$

where $m_v(t)$ is the envelope of voltage amplitude and $m_i(t)$ is the envelope of current amplitude. The average value of the instantaneous flicker power, which is simply called flicker power (FP), is expressed as follows:

$$FP = \frac{1}{T}\int_0^T fp(t)\,dt, \tag{6}$$

where T is the period time of the flicker. More details about flicker power measuring and monitoring are explained in [5].

2.4. Detection of the flicker sources using Jacobian matrix

In this section the flicker power sign of flicker sources that are simultaneously operated in a nonradial network is studied. An n-bus power system with m flicker sources is shown in Figure 4, where $m \leq n$. Since impedance and power demand of the flicker sources vary, voltage and current amplitudes fluctuate. The descriptive equations of the system can be obtained by node analysis. Effect of the power system topology, magnitude of the power system parameters, and properties of the supplied loads are given in these equations. In the system shown in Figure 4, amplitude of the bus voltages and load currents are functions of $R_1, R_2 \ldots R_m$.

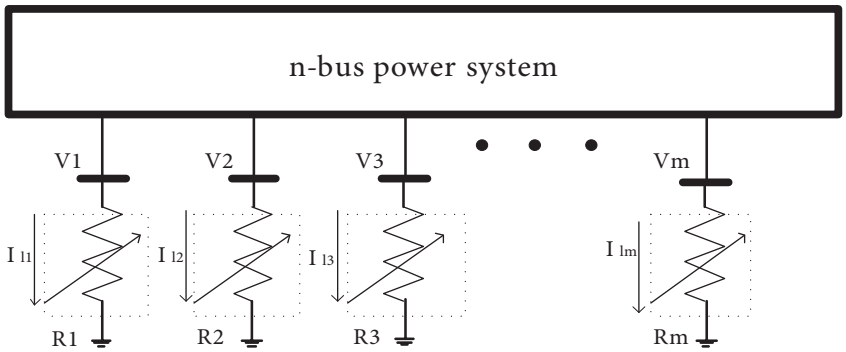

Figure 4. Power system with flicker sources.

For determining flicker power sign of loads, relative variation of the load voltages ($V_i(R_1, R_2, \ldots, R_m)\ i = 1, 2 \ldots m$) and load currents ($I_{li}(R_1, R_2, \ldots, R_m)\ i = 1, 2 \ldots m$) should be calculated. Since these are multivariable functions, the voltage and current gradients can be written as follows:

$$dV_i = \frac{\partial V_i}{\partial R_1}\,dR_1 + \frac{\partial V_i}{\partial R_2}\,dR_2 + \ldots + \frac{\partial V_i}{\partial R_m}\,dR_m\,;\ \ i = 1, 2, \ldots m, \tag{7}$$

$$dI_{Li} = \frac{\partial I_{Li}}{\partial R_1}\,dR_1 + \frac{\partial I_{Li}}{\partial R_2}\,dR_2 + \ldots + \frac{\partial I_{Li}}{\partial R_m}\,dR_m;\ \ i = 1, 2, \ldots m. \tag{8}$$

These equations can be shown in matrix form as follows:

$$\begin{bmatrix} \mathbf{\Delta V} \\ - \\ \mathbf{\Delta I_L} \end{bmatrix} = [\mathbf{J}]\ [\mathbf{\Delta R}], \tag{9}$$

or

$$\begin{bmatrix} \Delta V_1 \\ \Delta V_2 \\ \vdots \\ \Delta V_m \\ \Delta I_{l1} \\ \Delta I_{l2} \\ \vdots \\ \Delta I_{lm} \end{bmatrix} = \begin{bmatrix} \frac{\partial V_1}{\partial R_1} & \frac{\partial V_1}{\partial R_2} & \cdots & \frac{\partial V_1}{\partial R_m} \\ \frac{\partial V_2}{\partial R_1} & \frac{\partial V_2}{\partial R_2} & \cdots & \frac{\partial V_2}{\partial R_m} \\ \vdots & \vdots & \cdots & \vdots \\ \frac{\partial V_m}{\partial R_1} & \frac{\partial V_m}{\partial R_2} & \cdots & \frac{\partial V_m}{\partial R_m} \\ \frac{\partial I_{l1}}{\partial R_1} & \frac{\partial I_{l1}}{\partial R_2} & \cdots & \frac{\partial I_{l1}}{\partial R_m} \\ \frac{\partial I_{l2}}{\partial R_1} & \frac{\partial I_{l2}}{\partial R_2} & \cdots & \frac{\partial I_{l2}}{\partial R_m} \\ \vdots & \vdots & \cdots & \vdots \\ \frac{\partial I_{lm}}{\partial R_1} & \frac{\partial I_{lm}}{\partial R_2} & \cdots & \frac{\partial I_{lm}}{\partial R_m} \end{bmatrix} \begin{bmatrix} \Delta R_1 \\ \Delta R_2 \\ \vdots \\ \Delta R_m \end{bmatrix} . \tag{10}$$

$\boldsymbol{J}$ is the corresponding Jacobian matrix.

Impedance values are nonnegative; regarding this fact, some properties of the Jacobian matrix elements for $i = 1, 2 \ldots m$ and $j = 1, 2 \ldots m$ can be extracted as follows:

$$\frac{\partial V_i}{\partial R_j} > 0 , \tag{11}$$

$$\frac{\partial I_{li}}{\partial R_j} > 0 ; \; i \neq j \; , \tag{12}$$

$$\frac{\partial I_{li}}{\partial R_j} < 0 ; \; i = j \; , \tag{13}$$

$$\left| \frac{\partial I_{li}}{\partial R_i} \right| \geq \left| \frac{\partial I_{li}}{\partial R_j} \right| . \tag{14}$$

Flicker source impedances can vary related to another in 2^m modes. Without losing generality of the problem it is assumed that the number of the flicker sources is two ($m = 2$). At each moment, R_1 and R_2 can vary according to one of the following cases:

Case 1: $\Delta R_1 > 0, \; \Delta R_2 > 0 ,$

Case 2: $\Delta R_1 < 0, \; \Delta R_2 < 0 ,$

Case 3: $\Delta R_1 > 0, \; \Delta R_2 < 0 ,$

Case 4: $\Delta R_1 < 0, \; \Delta R_2 > 0 .$

In fact, these cases indicate the operation modes of the flicker sources. The cases can be presented by the phase angle of flicker tone such as that accomplished during the simulations. In the next step, for each case of flicker source operations, flicker power sign at loads is determined.

Case 1

- Since $\frac{\partial V_1}{\partial R_1} > 0$ and $\frac{\partial V_1}{\partial R_2} > 0$, then $\Delta V_1 > 0$. Also, $\frac{\partial I_{L1}}{\partial R_1} < 0$ and $\left| \frac{\partial I_{L1}}{\partial R_1} \right| \geq \left| \frac{\partial I_{L1}}{\partial R_2} \right|$, and then $\Delta I_{L1} < 0$. Therefore, at load-1 the flicker power is negative.

- Since $\frac{\partial V_2}{\partial R_1} > 0$ and $\frac{\partial V_2}{\partial R_2} > 0$, then $\Delta V_2 > 0$. Also, $\frac{\partial I_{L2}}{\partial R_2} < 0$ and $\left|\frac{\partial I_{L2}}{\partial R_2}\right| \geq \left|\frac{\partial I_{L2}}{\partial R_1}\right|$, and then $\Delta I_{L2} < 0$. Therefore, at load-2 flicker the power is negative.

Case 2

- Since $\frac{\partial V_1}{\partial R_1} > 0$ and $\frac{\partial V_1}{\partial R_2} > 0$, then $\Delta V_1 < 0$. Also, $\frac{\partial I_{L1}}{\partial R_1} < 0$ and $\left|\frac{\partial I_{L1}}{\partial R_1}\right| \geq \left|\frac{\partial I_{L1}}{\partial R_2}\right|$, and then $\Delta I_{L1} > 0$. Therefore, at load-1 the flicker power is negative.
- Since $\frac{\partial V_2}{\partial R_1} > 0$ and $\frac{\partial V_2}{\partial R_2} > 0$, then $\Delta V_2 < 0$. Also, $\frac{\partial I_{L2}}{\partial R_2} < 0$ and $\left|\frac{\partial I_{L2}}{\partial R_2}\right| \geq \left|\frac{\partial I_{L2}}{\partial R_1}\right|$, and then $\Delta I_{L2} > 0$. Therefore, at load-2 the flicker power is negative.

Case 3

- If $\left|\frac{\partial V_1}{\partial R_1}\right| > \left|\frac{\partial V_1}{\partial R_2}\right|$, since $\frac{\partial V_1}{\partial R_1} > 0$ and $\frac{\partial V_1}{\partial R_2} > 0$, then $\Delta V_1 > 0$. Also, $\frac{\partial I_{L1}}{\partial R_1} < 0$ and $\frac{\partial I_{L1}}{\partial R_2} > 0$, and then $\Delta I_{L1} < 0$. Therefore, at load-1 the flicker power is negative.
- If $\left|\frac{\partial V_1}{\partial R_1}\right| < \left|\frac{\partial V_1}{\partial R_2}\right|$, since $\frac{\partial V_1}{\partial R_1} > 0$ and $\frac{\partial V_1}{\partial R_2} > 0$, then $\Delta V_1 < 0$. Also, $\frac{\partial I_{L1}}{\partial R_1} < 0$ and $\frac{\partial I_{L1}}{\partial R_2} > 0$, and then $\Delta I_{L1} < 0$. Therefore, at load-1 the flicker power is positive.
- If $\left|\frac{\partial V_2}{\partial R_1}\right| > \left|\frac{\partial V_2}{\partial R_2}\right|$, since $\frac{\partial V_2}{\partial R_1} > 0$ and $\frac{\partial V_2}{\partial R_2} > 0$, then $\Delta V_2 > 0$. Also, $\frac{\partial I_{L2}}{\partial R_1} > 0$ and $\frac{\partial I_{L2}}{\partial R_2} < 0$, and then $\Delta I_{L2} > 0$. Therefore, at load-2 the flicker power is positive.
- If $\left|\frac{\partial V_2}{\partial R_1}\right| < \left|\frac{\partial V_2}{\partial R_2}\right|$, since $\frac{\partial V_2}{\partial R_1} > 0$ and $\frac{\partial V_2}{\partial R_2} > 0$, then $\Delta V_2 < 0$. Also, $\frac{\partial I_{L2}}{\partial R_1} > 0$ and $\frac{\partial I_{L2}}{\partial R_2} < 0$, and then $\Delta I_{L2} > 0$. Therefore, at load-2 the flicker power is negative.

Case 4

- If $\left|\frac{\partial V_1}{\partial R_1}\right| > \left|\frac{\partial V_1}{\partial R_2}\right|$, since $\frac{\partial V_1}{\partial R_1} > 0$ and $\frac{\partial V_1}{\partial R_2} > 0$, then $\Delta V_1 < 0$. Also, $\frac{\partial I_{L1}}{\partial R_1} < 0$ and $\frac{\partial I_{L1}}{\partial R_2} > 0$, and then $\Delta I_{L1} > 0$. Therefore, at load-1 the flicker power is negative.
- If $\left|\frac{\partial V_1}{\partial R_1}\right| < \left|\frac{\partial V_1}{\partial R_2}\right|$, since $\frac{\partial V_1}{\partial R_1} > 0$ and $\frac{\partial V_1}{\partial R_2} > 0$, then $\Delta V_1 > 0$. Also, $\frac{\partial I_{L1}}{\partial R_1} < 0$ and $\frac{\partial I_{L1}}{\partial R_2} > 0$, and then $\Delta I_{L1} > 0$. Therefore, at load-1 the flicker power is positive.
- If $\left|\frac{\partial V_2}{\partial R_1}\right| > \left|\frac{\partial V_2}{\partial R_2}\right|$, since $\frac{\partial V_2}{\partial R_1} > 0$ and $\frac{\partial V_2}{\partial R_2} > 0$, then $\Delta V_2 < 0$. Also, $\frac{\partial I_{L2}}{\partial R_1} > 0$ and $\frac{\partial I_{L2}}{\partial R_2} < 0$, and then $\Delta I_{L2} < 0$. Therefore, at load-2 the flicker power is positive.
- If $\left|\frac{\partial V_2}{\partial R_1}\right| < \left|\frac{\partial V_2}{\partial R_2}\right|$, since $\frac{\partial V_2}{\partial R_1} > 0$ and $\frac{\partial V_2}{\partial R_2} > 0$, then $\Delta V_2 > 0$. Also, $\frac{\partial I_{L2}}{\partial R_1} > 0$ and $\frac{\partial I_{L2}}{\partial R_2} < 0$, and then $\Delta I_{L2} < 0$. Therefore, at load-2 the flicker power is negative.

These results can be summarized as follows. When impedance magnitudes of the flicker sources vary similarly together, such as in cases 1 and 2, the flicker power sign at these loads becomes negative. In other words, when flicker sources operate with similar phase angles, the flicker power at contaminative loads is

negative. When impedance magnitudes of the flicker sources vary dissimilarly together, such as in cases 3 and 4, the flicker power sign at these loads will become negative if $\left|\frac{\partial V_1}{\partial R_1}\right| > \left|\frac{\partial V_1}{\partial R_2}\right|$ and $\left|\frac{\partial V_2}{\partial R_1}\right| < \left|\frac{\partial V_2}{\partial R_2}\right|$. These two conditions mean that the sensitivity of a bus voltage to its load is higher than that of the other bus loads. These two conditions are usually satisfied in real power systems. Therefore, contaminative loads can be detected by measuring flicker power at their supplying point.

In the next section, flicker propagation throughout the power network is investigated and a method for dominant source identification based on propagation circumstances is proposed.

3. Flicker propagation and dominant source identification

In this section flicker propagation throughout the power system is investigated. Instantaneous bus voltages and transmission line currents are utilized. Direction of the active power flow is assumed to be given in the transmission lines. Consider the situations shown in Figures 5 and 6. Two different situations will occur depending on the location of the flicker source, upstream or downstream of the monitoring point (the point where voltage and current are measured and flicker power is calculated).

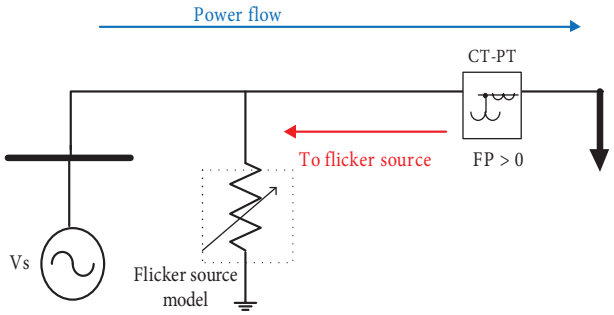

Figure 5. Flicker source is located upstream of the monitoring point; flicker power is positive.

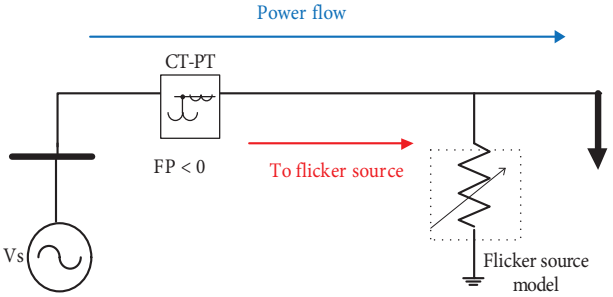

Figure 6. Flicker source is located downstream of the monitoring point; flicker power is negative.

If the flicker source is located upstream, in the monitoring point, the fluctuation of the voltage amplitude will follow the fluctuation of the current amplitude. The envelope signal in the voltage and current will be in phase. Therefore, flicker power, which is calculated in the monitoring point, is positive. As shown in Figure 5, in this situation (when flicker power is positive), direction of movement from monitoring point to flicker source is not the same as the direction of active power flow. In other words, to get the flicker source from the monitoring point, movement should be the opposite of the direction of the active power flow.

If the flicker source is located downstream, at the monitoring point, the voltage and current envelopes are in opposite phases since an increase in current will lead to a decrease in voltage. Therefore, flicker power, which is calculated at the monitoring point, is negative. As shown in Figure 6, in this situation (when flicker power is negative), direction of movement from monitoring point to flicker source is the same as the active power flow direction. In other words, to get the flicker source from the monitoring point, movement should be similar to the active power flow direction.

From these two situations, we conclude that the flicker power sign will differ depending on the location of the flicker source. Thus, it must be possible to develop an algorithm for employing this information to identify the dominant flicker source (or sources).

3.1. Dominant flicker source identification by directed graph theory

In this section, to identify the dominant flicker source, for analyzing information such as flicker power sign and active power flow direction in the transmission lines a directed graph theory is applied. A special defined directed graph is introduced for this aim. Power system buses are considered as vertices and transmission lines are considered as edges (arcs) of the proposed directed graph. For defining the direction of the arcs and constructing the corresponding adjacency matrix, two different possible conditions for two neighboring buses (bus-i and bus-j) of the power system are considered as shown in Figures 7 and 8. Direction of the arcs indicates flicker source location.

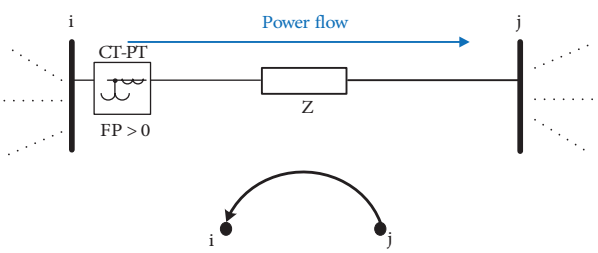

Figure 7. Determining direction of the arc between two vertices; flicker power is positive at monitoring point.

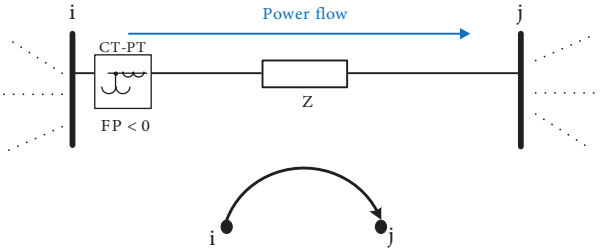

Figure 8. Determining direction of the arc between two vertices; flicker power is negative at monitoring point.

In the first condition, demonstrated in Figure 7, the flicker power at the monitoring point (bus-i) is positive. Assume that active power flows from bus-i to bus-j. According to the previous discussion, flicker propagates from bus-i to bus-j. Since the direction of each arc indicates the flicker source, the arc, which corresponds to this transmission line, is from vertex-j to vertex-i. In the second condition, the active power flow direction is similar to the previous case while the flicker power at the monitoring point (bus-i) is negative, as shown in Figure 8. Therefore, flicker propagates from bus-j to bus-i. In the proposed directed graph, the arc, which is corresponds to this transmission line, is from vertex-i to vertex-j.

The proposed adjacency matrix $\mathbf{A}$ is an $n \times n$ matrix where n is the number of power system buses or number of directed graph vertices. The adjacency matrix is constructed as follows:

- If two buses such as bus-i and bus-j are connected together by a transmission line, then an arc will exist between vertex-i and vertex-j in the corresponding directed graph. In this condition, if the arc direction is from vertex-i to vertex-j, then $a_{ij} = -a_{ji} = 1$, and if the arc direction is from vertex-j to vertex-i, then $a_{ij} = -a_{ji} = -1$.

- If two buses such as bus-i and bus-j are not connected together by a transmission line, then an arc will not exist between vertex-i and vertex-j in the corresponding directed graph. In this condition, $a_{ij} = a_{ji} = 0$.

- Main diagonal elements of the adjacency matrix are one; $a_{ii} = 1$; $i = 1, 2, \ldots, n$.

3.1.1. Dominant flicker source identification from the proposed directed graph

If the direction of all arcs connected to vertex-i is from different vertices to vertex-i, then bus-i will be diagnosed as the location of the dominant flicker source. In other words, bus-i will be the location of the dominant flicker source if each arc connected to vertex-i shows this vertex as the flicker source.

3.1.2. Dominant flicker source identification from the adjacency matrix of the directed graph

If all elements of the ith column of the adjacency matrix are nonnegative, then vertex-i will indicate the bus (bus-i) where the dominant flicker source has been coupled. Figure 9 gives a general outline of an algorithm that is used to identify the coupling point (bus number) of the dominant flicker source from the adjacency matrix, as explained above.

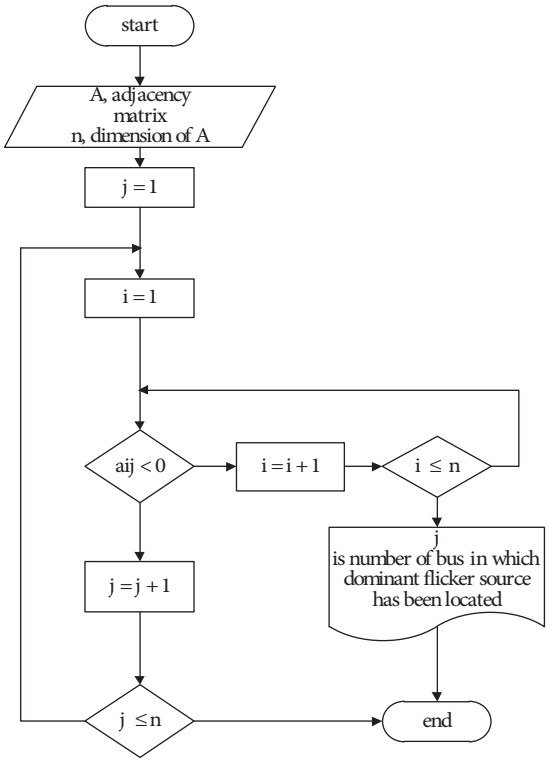

Figure 9. Flowchart for identifying dominant flicker source location from adjacency matrix.

After measuring instantaneous bus voltages and line currents, this method can identify the dominant flicker source or sources in the power system. In this paper it is assumed that flicker sources are equal in size and power demand and then the effect of their locations and operation modes on the dominance is investigated.

3.2. Effect of the flicker source locations and operation modes on dominance

Consider two buses of the power system supply as two similarly sized flicker sources as shown in Figure 10. Without losing generality of the problem, this situation can be exchanged to a simple power system as shown in Figure 11.

According to Figure 11, Z, Z_s, and Z_l are impedances of the system. R_1 and R_2 are variable impedance of the flicker sources. I is the current of the linear load supplied by bus-1. I_1 and I_2 are currents of the nonlinear loads, which act as flicker sources. At the monitoring point, transmission line current (i) and bus-2 voltage (V_2) are measured and flicker power is calculated. Amplitudes of the measured current and voltage are functions of the nonlinear load impedances and their gradients can be written as below.

$$dV_2 = \frac{\partial V_2}{\partial R_1}\, dR_1 + \frac{\partial V_2}{\partial R_2}\, dR_2 \tag{15}$$

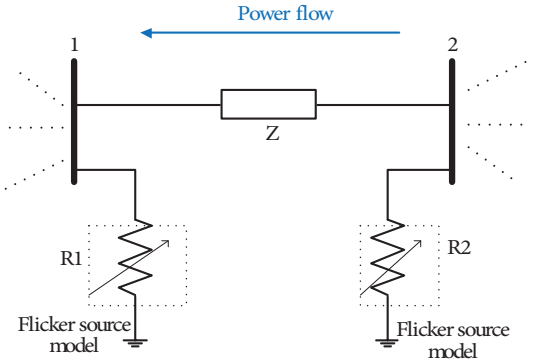

Figure 10. Two similar flicker sources that are connected to different buses.

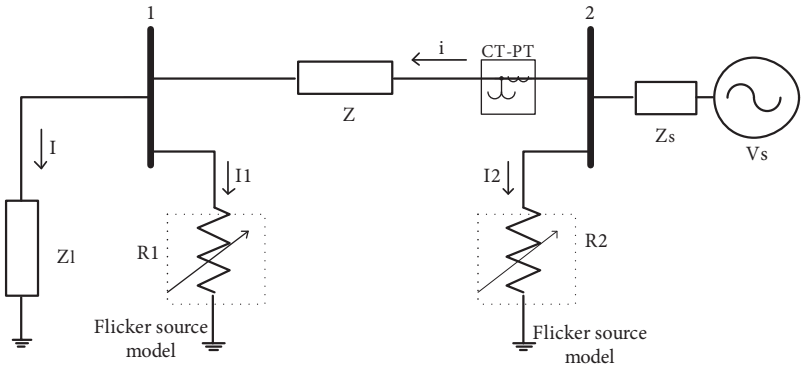

Figure 11. Simplified system of Figure 10.

$$di = \frac{\partial i}{\partial R_1}\, dR_1 + \frac{\partial i}{\partial R_2}\, dR_2 \tag{16}$$

These equations can be shown in matrix form as follows.

$$\begin{bmatrix} \Delta V_2 \\ \Delta i \end{bmatrix} = \begin{bmatrix} \frac{\partial V_2}{\partial R_1} & \frac{\partial V_2}{\partial R_2} \\ \frac{\partial i}{\partial R_1} & \frac{\partial i}{\partial R_2} \end{bmatrix} \begin{bmatrix} \Delta R_1 \\ \Delta R_2 \end{bmatrix} \tag{17}$$

Impedance values are nonnegative; regarding this fact, some properties of the Jacobian matrix elements can be extracted as follows.

$$\frac{\partial V_2}{\partial R_1} > 0 \tag{18}$$

$$\frac{\partial V_2}{\partial R_2} > 0 \tag{19}$$

$$\frac{\partial i}{\partial R_2} > 0 \tag{20}$$

$$\frac{\partial i}{\partial R_1} < 0 \tag{21}$$

$$\frac{\partial V_2}{\partial R_2} > \frac{\partial V_2}{\partial R_1} \tag{22}$$

Mathematically the magnitude of $\frac{\partial i}{\partial R_1}$ can be larger or smaller than the magnitude of $\frac{\partial i}{\partial R_2}$. If $Z_L \ll R_1$ then $\left|\frac{\partial i}{\partial R_1}\right| < \left|\frac{\partial i}{\partial R_2}\right|$. This condition is not satisfied in power systems. Therefore, usually $\left|\frac{\partial i}{\partial R_1}\right| > \left|\frac{\partial i}{\partial R_2}\right|$.

At each moment, R_1 and R_2 can vary according to one of the cases described in Section 3. In the next step, for each case, flicker power sign is determined at the monitoring point.

Case 1

- Since $\frac{\partial V_2}{\partial R_1} > 0$ and $\frac{\partial V_2}{\partial R_2} > 0$, then $\Delta V_2 > 0$. Also, $\frac{\partial i}{\partial R_1} < 0$ and $\left|\frac{\partial i}{\partial R_1}\right| \geq \left|\frac{\partial i}{\partial R_2}\right|$, and then $\Delta i < 0$. Therefore, at the monitoring point flicker power is negative. It means that the dominant source has been located downstream; source-1 is dominant.

Case 2

- Since $\frac{\partial V_2}{\partial R_1} > 0$ and $\frac{\partial V_2}{\partial R_2} > 0$, then $\Delta V_2 < 0$. Also, $\frac{\partial i}{\partial R_1} < 0$ and $\left|\frac{\partial i}{\partial R_1}\right| \geq \left|\frac{\partial i}{\partial R_2}\right|$, and then $\Delta i > 0$. Therefore, at the monitoring point flicker power is negative. It means that the dominant source has been located downstream; source-1 is dominant.

Case 3

- Since $\frac{\partial V_2}{\partial R_1} > 0$, $\frac{\partial V_2}{\partial R_2} > 0$, and $\frac{\partial V_2}{\partial R_2} > \frac{\partial V_2}{\partial R_1}$, then $\Delta V_2 < 0$. Also, $\frac{\partial i}{\partial R_1} < 0$ and $\frac{\partial i}{\partial R_2} > 0$, and then $\Delta i < 0$. Therefore, at the monitoring point flicker power is positive. It means that the dominant source has been located upstream; source-2 is dominant.

Case 4

- Since $\frac{\partial V_2}{\partial R_1} > 0$, $\frac{\partial V_2}{\partial R_2} > 0$ and $\frac{\partial V_2}{\partial R_2} > \frac{\partial V_2}{\partial R_1}$, then $\Delta V_2 > 0$. Also, $\frac{\partial i}{\partial R_1} < 0$ and $\frac{\partial i}{\partial R_2} > 0$, and then $\Delta i > 0$. Therefore, at the monitoring point flicker power is positive. It means that the dominant source has been located upstream; source-2 is dominant.

Finally the results of the discussed cases can be summarized in this manner: when the flicker sources operate in phase, the source located downstream (relative to the monitoring point) becomes the dominant source. When the flicker sources operate in the opposite phase, the source located upstream (relative to the monitoring point) becomes the dominant source.

4. Evaluation of the proposed methods by simulating

For evaluating the proposed methods some simulations are conducted. A typical six-bus nonradial power system is studied. Several flicker sources are simultaneously operated in the chosen power system. For both the single point method and the directed graph-based method some different scenarios are suggested. In these scenarios the number, power demand, coupling points, and operation modes of the flicker sources are changed, but in each simulation, fluctuation frequency of the flicker sources is assumed to be equal.

4.1. System model

In this paper a typical six-bus power system with nominal frequency of 50 Hz and nominal voltage of 230 KV is studied, as shown in Figure 12. The power system data are presented in the Appendix.

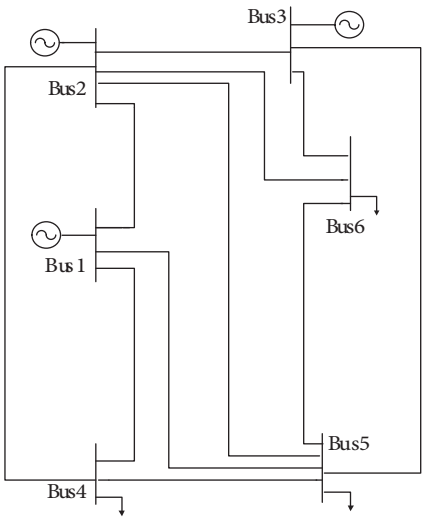

Figure 12. Studied 6-bus power system.

In conducted simulations a spot welding machine is considered as the flicker source. Several of these machines are distributed throughout the network. Operation of the spot welding machines causes fluctuating voltage and current amplitudes. In other words, these machines act as contaminative loads in the power system. A spot welding machine is modeled as a resistor connected to an ideal switch. Magnitude of the resistor indicates power demand of the contaminative load. In this model of the flicker source, by changing the resistance value, the amplitude of flicker tone varies and the switching frequency determines the frequency of the flicker tone. Since flicker sources with similar frequencies are investigated in this paper, in each scenario that is simulated, fluctuation frequencies of all flicker sources are equal. The welding machine model and the connection of it to the power system at the jth bus are shown in Figure 13. In addition to the nonlinear load, this bus may supply other linear loads or be connected to a power station, as demonstrated in Figure 13.

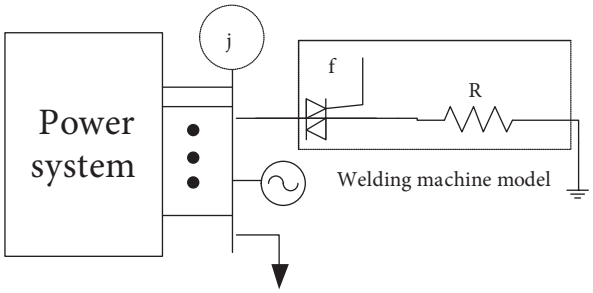

Figure 13. Connection of the nonlinear load as flicker source to bus-j.

4.2. Single point method simulation results

According to the proposed theory discussed and derived in Section 3, at flicker sources (nonlinear loads causing voltage fluctuation), flicker power is negative, and at linear loads, flicker power is positive. This result can be considered as a criterion to detect the contaminative loads and determine the buses that supply flicker sources, thus identifying flicker source locations. For this purpose, load instantaneous currents and bus instantaneous voltages are required and should be monitored. Then, at each branch connected to a bus, flicker power is calculated.

For evaluating this criterion, five scenarios are suggested and simulated. Details of the scenarios are explained in Table 1. In each scenario several dissimilar flicker sources with different power demands are assumed to be connected to the power system. Despite differences in power demand of the flicker sources, these spot welding machines act intermittently in equal frequency, producing flickers at the same frequency. Although flicker sources are nonlinear loads, in addition to these loads other nonlinear loads, whose currents contain harmonics, have been assumed to operate in the power system in scenarios 1 and 2.

Table 1. Details of the simulated scenarios; single point method.

Scenario	Flicker sources located buses	Properties of the spot welding machines	
		Resistance (p.u.)	Frequency (Hz)
1	2	6.61	10
	4	1.6	10
2	1	1.6	8
	6	1.89	8
3	3	6.61	13
	5	1.89	13
4	5	6.61	9
	6	1.89	9
5	3	6.61	11
	4	1.6	11
	6	1.89	11

Although fluctuation frequency of the contaminative loads is equal, start times of their intermittency may not be equal. It is possible the spot welding machines are operated with time delay relatively together (spot welding machines are not synchronous necessarily). In other words, flicker sources can be operated in different modes. This fact is revealed in the difference of the phase angles of the voltage envelopes. To consider the effect of the phase angle (operation mode) on identified sources, each scenario is simulated for different operation modes.

For scenario 1, flicker power at each branch connected to the power system buses is presented in Table 2. This scenario is simulated for three operation modes (θ_i indicates the phase angle of the voltage envelope produced by the spot welding machine coupled to bus-i). In all operation modes, the flicker power sign shows contaminative loads. Note that the power system voltage and power are respectively 230 KV and 100 MW.

In this scenario a nonlinear load (harmonic load) has been supplied by bus 5. To model the nonlinear load, three controlled current sources have been connected to bus 5 parallel with the load of the bus. The controlled sources inject currents with harmonic order 5, 7, and 11 to the system at bus 5. Amplitude of the currents is respectively 10%, 8%, and 5% of the fundamental frequency component absorbed by the load. The load with the current sources models the nonlinear load (harmonic load) totally.

The results show that for loads (linear or nonlinear) that are not flicker sources, flicker power is positive. In other words, the presence of harmonic nonlinear loads does not affect the performance of the proposed method.

Tables 3 and 4 show results corresponding to scenarios 2 and 3. Similarly in these scenarios, for different flicker source operation times (different operation modes), flicker power is negative at each flicker source branch. Therefore, the proposed criterion is successful in detecting the contaminative loads.

Table 2. Flicker power at branch connected to buses; scenario 1.

Bus and branch		Operation mode of the flicker sources					
		1		2		3	
		θ_2°	θ_4°	θ_2°	θ_4°	θ_2°	θ_4°
		0	0	60	0	285	0
1	G1	4.58e4		3.98e4		3.56e4	
2	G2	2.32e4		2.06e4		1.77e4	
	Flicker source	–4.13e4		–2.90e4		–1.58e4	
3	G3	2.28e4		1.97e4		1.73e4	
4	Linear load	3.78e4		3.46e4		2.98e4	
	Flicker source	–1.77e5		–1.67e5		–1.56e5	
5	Nonlinear load	2.85e4		2.57e4		2.18e4	
6	Linear load	2.72e4		2.46e4		2.06e4	

Table 3. Flicker power at branch connected to buses; scenario 2.

Bus and branch		Operation mode of the flicker sources					
		1		2		3	
		θ_1°	θ_6°	θ_1°	θ_6°	θ_1°	θ_6°
		0	0	30	0	210	0
1	G1	1.08e5		1.08e5		1.17e4	
	Flicker source	–2.65e5		–2.46e5		–6.19e4	
2	G2	4.57e4		4.22e4		3712	
3	G3	5.32e4		4.85e4		4381	
4	Nonlinear load	6.34e4		5.90e4		4902	
5	Linear load	6.31e4		5.81e4		4853	
6	Linear load	6.80e4		6.11e4		6119	
	Flicker source	–1.88e5		–1.77e5		–1.55e4	

In scenario 2, the linear load of bus 4 has been changed to a nonlinear load, similarly to scenario 1. The results show that the method can make a distinction between flicker sources and harmonic load.

If the power system is in the situation suggested in scenario 4, flicker power magnitude at bus branches will be equal to that presented in Table 5. In this scenario, flicker power at contaminative load branches is negative and the criterion is confirmed again.

Table 4. Flicker power at branch connected to buses; scenario 3.

Bus and branch		Operation mode of the flicker sources					
		1		2		3	
		θ_3°	θ_5°	θ_3°	θ_5°	θ_3°	θ_5°
		0	0	45	0	270	0
1	G1	3.46e4		3.05e4		2.38e4	
2	G2	1.8e4		1.58e4		1.21e4	
3	G3	0.27e4		1.98e4		1.46e4	
	Flicker source	–3.87e4		–2.8e4		–1.11e4	
4	Linear load	2.39e4		2.12e4		1.66e4	
5	Linear load	3.01e4		2.69e4		2.16e4	
	Flicker source	–1.36e5		–1.28e5		–1.12e5	
6	Linear load	2.55e4		2.26e4		1.72e4	

Table 5. Flicker power at branch connected to buses; scenario 4.

Bus and branch		Operation mode of the flicker sources					
		1		2		3	
		$\theta_5{}^\circ$	$\theta_6{}^\circ$	$\theta_5{}^\circ$	$\theta_6{}^\circ$	$\theta_5{}^\circ$	$\theta_6{}^\circ$
		0	0	90	0	300	0
1	G1	2.93e4		1.91e4		2.42e4	
2	G2	1.65e4		1.1e4		1.38e4	
3	G3	2.16e4		1.46e4		1.82e4	
4	Linear load	2.12e4		1.41e4		1.76e4	
5	Linear load	2.41e4		1.58e4		1.96e4	
	Flicker source	–3.36e4		–7049		–2.24e4	
6	Linear load	2.76e4		1.89e4		2.35e4	
	Flicker source	–1.28e5		–1.05e5		–1.15e5	

In the fifth scenario three spot welding machines are distributed throughout the network and each flicker source is connected to a bus. Four different situations for phase angle of the envelope signals are simulated. In all situations the flicker power sign correctly shows contaminative loads and their supplying bus as given in Table 6.

4.3. The results of simulations for directed graph-based method

In this section the proposed method presented in Section 4 is simulated. For evaluating these methods, three scenarios are suggested and simulated. Details of the scenarios are explained in Table 7. In order to focus on the effect of the location and operation mode of the flicker sources on dominancy, power demands of the spot welding machines are considered equal at each scenario.

Table 6. Flicker power at branch connected to buses; scenario 5.

Bus and branch		Operation mode of the flicker sources											
		1			2			3			4		
		θ_3°	θ_4°	θ_6°	θ_3°	θ_4°	θ_6°	θ_3°	θ_4°	θ_6°	θ_3°	θ_4°	θ_6°
		0	0	0	60	30	0	300	60	0	45	180	0
1	G1	1.05e5			9.36e4			6.35e4			986		
2	G2	5.6e4			4.97e4			3.32e4			384		
3	G3	6.67e4			5.85e4			3.77e4			1040		
	Flicker source	–6.08e4			–4.49e4			–7996			–7626		
4	Linear load	8.47e4			7.86e4			5.43e4			1423		
	Flicker source	–2.46e5			–2.31e5			–1.66e5			–2.04e4		
5	Linear load	7.54e4			6.82e4			4.58e4			611		
6	Linear load	8.2e4			7.36e4			4.92e4			1207		
	Flicker source	–2.02e5			–1.8e5			–1.51e5			–2.27e4		

Table 7. Details of the simulated scenarios; directed graph based method.

Scenario	Flicker sources located buses	Properties of the spot welding machines	
		Resistance (p.u.)	Frequency (Hz)
1	5	1.32	15
2	2	1.32	12
	5		
3	1	1.88	10
	4		
	6		

In the first scenario a spot welding machine as a flicker source is connected to bus-5. Active power flow direction on transmission lines of the power system is independent of the start time of the spot welding machines. Therefore, for different operation modes, power flow direction remains constant. Power flow direction at each line is presented in Table 8. This scenario is simulated for four different operation modes. Each situation indicates a phase angle of the voltage envelope signal. Calculated flicker power at the monitoring points is presented in Table 8. At a certain monitoring point, for all operational modes, calculated flicker powers have the same sign. Therefore, directed graphs corresponding to the situations are equal and shown in Figure 14. As demonstrating in Figure 14, vertex-5 is the vertex that all connected arcs arrived to. Except for vertex-5, there is no vertex that all arcs that have been connected to show as a flicker source. Therefore, regarding this graph, bus-5 is diagnosed as the location of the dominant flicker source. The adjacency matrix corresponding to this graph is constructed according to the proposed structure defined in Section 4, as below.

$$\begin{bmatrix} 1 & 1 & 0 & 1 & 1 & 0 \\ -1 & 1 & 1 & -1 & 1 & 1 \\ 0 & -1 & 1 & 0 & 1 & -1 \\ -1 & 1 & 0 & 1 & 1 & 0 \\ -1 & -1 & -1 & -1 & 1 & -1 \\ 0 & -1 & 1 & 0 & 1 & 1 \end{bmatrix}.$$

As expected, elements of the fifth column of the adjacency matrix are nonnegative. In addition to diagnosing the dominant source from the graph, its location can be found from this matrix.

Table 8. Flicker power and power flow direction at transmission lines; scenario 1.

Line	Power flow direction		Operation mode of the flicker source			
			1	2	3	4
	From bus	To bus	θ_5°	θ_5°	θ_5°	θ_5°
			0	60	180	210
1	1	2	–5833	–5619	–5742	–5727
2	1	4	–1171	–1209	–1293	–913
3	1	5	–3.27e4	–3.18e4	–3.16e4	–3.26e4
4	2	3	–3054	–2834	–3048	–3269
5	2	4	9522	9314	8996	9525
6	2	5	–2.73e4	–2.66e4	–2.6e4	–2.71e4
7	2	6	–2008	–1908	–2060	–1985
8	3	5	–2.94e4	–2.88e4	–2.81e4	–2.89e4
9	3	6	750	768	593	961
10	4	5	–2.54e4	–2.46e4	–2.44e4	–2.52e4
11	6	5	–2.21e4	–2.17e4	–2.04e4	–2.16e4

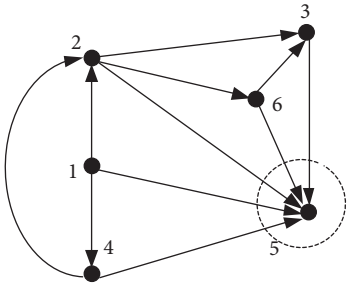

Figure 14. Directed graph corresponding to scenario 1.

In the second scenario two similar flicker sources (two spot welding machines with equal power demand and switching frequency) operate in the power system. Note that the start time of the machines is not necessarily equal. One of them is connected to bus-5 and other one is supplied by bus-2. Results of simulating the power system in this scenario for different operation modes of the flicker sources are given in Table 9. Corresponding directed graphs are shown in Figure 15. For mode-1 and mode-2, the flicker source located in bus-5 is diagnosed as the dominant flicker source. For mode-3 and mode-4, the flicker source located in bus-2 is diagnosed as the dominant flicker source. These results confirm the theory presented in Section 4. For mode-1 and mode-2, flicker sources are in phase. Therefore, the flicker source located downstream should be diagnosed as the dominant source. Bus-5 is downstream relative to bus-2. It is diagnosed correctly as the location of the dominant source. For mode-3 and mode-4 flicker sources are in opposite phases. Therefore, the flicker source located upstream should be diagnosed as the dominant source. Bus-2 is upstream relative to bus-5. It is diagnosed as the location of the dominant source.

In the third scenario three spot welding machines, as flicker sources, are assumed to be connected to bus-1, bus-2, and bus-6. For modeling the temporal difference of the start time of the machines, four operational modes are simulated. Calculated flicker power at monitoring points and active power flow direction are presented in Table 10. Corresponding directed graphs are shown in Figure 16. For mode-1 and mode-2, flicker sources located in bus-4 and bus-6 are diagnosed as dominant flicker sources. In these modes flicker sources operate in phase. The reason for the dominancy of bus-4 against bus-1 is that active power flows from bus-1 to bus-4, and

when the flicker sources are operated in phase, the source located downstream becomes the dominant source. For mode-3, flicker sources located in bus-1 and bus-6 are diagnosed as dominant flicker sources. In this mode, flicker sources located in bus-1 and bus-4 are operated in opposite phases. When the flicker sources are operated in opposite phases, the source located upstream becomes the dominant source. Therefore, bus-1 is dominant compared to bus-4. For mode-4, the flicker source located in bus-1 is diagnosed as the dominant flicker source.

Table 9. Flicker power and power flow direction at transmission lines; scenario 2.

Line	Power flow direction		Operation mode of the flicker sources							
			1		2		3		4	
	From bus	To bus	θ_2°	θ_5°	θ_2°	θ_5°	θ_2°	θ_5°	θ_2°	θ_5°
			0	0	0	60	0	180	0	210
1	1	2	–6.69e4		–4.97e4		–90.99		–2506	
2	1	4	–1.82e4		–1.41e4		–12		–405	
3	1	5	–6.02e4		–4.59e4		54		–3620	
4	3	2	–3.57e4		–2.69e4		–2575		–3785	
5	2	4	8.61e4		6.38e4		2326		5372	
6	2	5	–1.43e4		–8611		3592		444	
7	2	6	3.66e4		2.75e4		1758		2246	
8	3	5	–4.84e4		–3.71e4		391		–2625	
9	3	6	5978		2484		2		789	
10	4	5	–3.61e4		–2.82e4		774		–1071	
11	6	5	–2.75e4		–2.31e4		–2861		–4547	

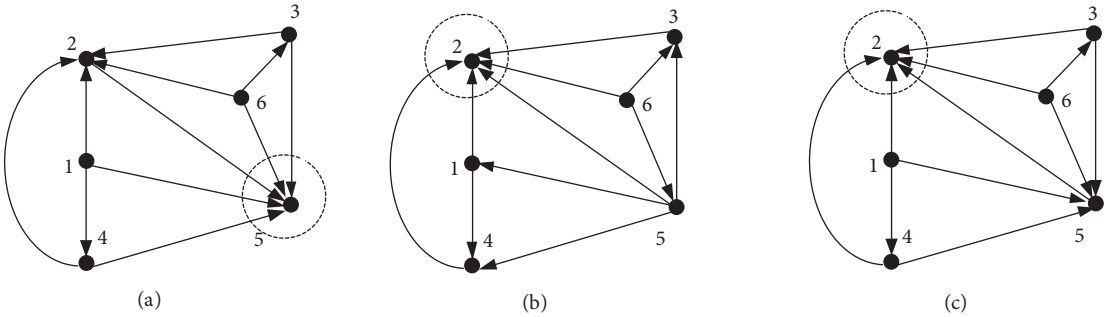

Figure 15. Directed graph corresponding to scenario 2: (a) modes 1 and 2, (b) mode 3, (c) mode 4.

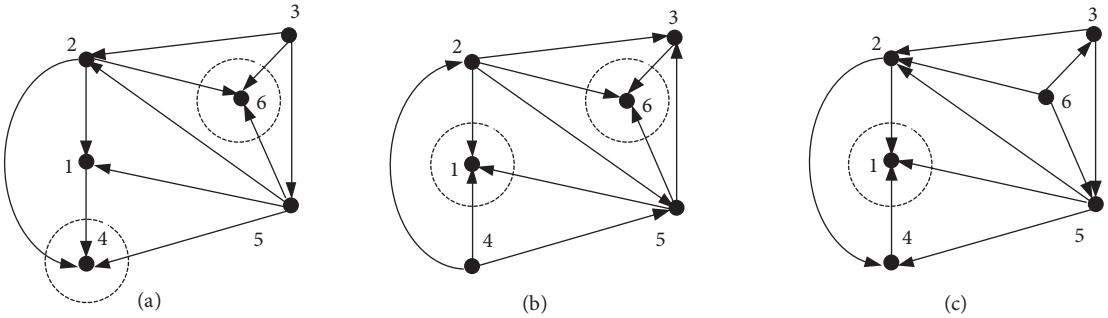

Figure 16. Directed graph corresponding to scenario 3: (a) modes 1 and 2, (b) mode 3, (c) mode 4.

Table 10. Flicker power and power flow direction at transmission lines; scenario 3.

Line	Power flow direction		Operation mode of the flicker sources											
			1			2			3			4		
	From bus	To bus	θ_1°	θ_4°	θ_6°	θ_1°	θ_4°	θ_6°	θ_1°	θ_4°	θ_6°	θ_1°	θ_4°	θ_6°
			0	0	0	0	30	60	0	180	45	0	30	210
1	1	2	2.48e4			2.22e4			8422			2.99e4		
2	1	4	–8778			–6647			3.12e4			5188		
3	1	5	3.03e4			2.86e4			4617			2.54e4		
4	3	2	–8218			–8971			9208			–1.36e4		
5	2	4	–7.01e4			–6.46e4			3.53e4			–4.42e4		
6	2	5	7904			7213			–1817			2274		
7	2	6	–1.38e4			–6615			–2.01e4			2.95e4		
8	3	5	–3297			–3671			5233			–1e4		
9	3	6	–6.33e4			–4.86e4			–2.61e4			1.82e4		
10	4	5	2.49e4			2.43e4			–5737			1.32e4		
11	5	6	–2.18e4			–1.54e4			–1.33e4			1.78e4		

5. Conclusion

In this paper, first a theory based on the Jacobian matrix of the considered power system is developed to propose a single point method for detecting flicker sources. This method employs the result of the analytical theory as a criterion. This criterion is expressed by the flicker power sign; flicker power at contaminative load is negative. In the second step, propagation of the flicker throughout the network is investigated to identify the dominant flicker source. For this purpose, after calculating flicker power and measuring the direction of the active power flow at monitoring points, the mutual relation between calculated flicker power signs and power flow directions is utilized to identify dominant flicker source. An algorithm based on a special defined directed graph is proposed to analyze these two parameters mutually. The dominant flicker source can be identified by this graph or its corresponding adjacency matrix. Location and operation mode of the flicker sources as two main factors for dominancy of a flicker source are analytically investigated and then the criteria are obtained for diagnosing and justifying dominant flicker sources. The proposed methods are simulated in a typical nonradial power system for different scenarios. Simulation results verified the proposed criteria and methods.

References

[1] Baggini A. Handbook of Power Quality. New York, NY, USA: Wiley, 2008.

[2] Ammar M, Joos G. Impact of distributed wind generators reactive power behavior on flicker severity. IEEE T Energy Conver 2013; 28: 425–433.

[3] IEC. Standard 61000-4-15. Flickermeter—Functional and Design Specifications. Geneva, Switzerland: IEC, 2003.

[4] Wiczynski G. Inaccuracy of short-term light flicker P_{st} indicator measuring with a flickermeter. IEEE T Power Deliver 2012; 27: 2428–2430.

[5] Axelberg PGV, Bollen MHJ. Trace of flicker source by using the quantity of flicker power. IEEE T Power Deliver 2008; 23: 465–471.

[6] Nassif AB, Nino EE, Xu W. A V-I slope-based method for flicker source detection. In: 37th Power Symposium Annual North American; 23–25 October 2005; Ames, IA, USA. New York, NY, USA: IEEE. pp. 755–760.

[7] Morsi WG, El-Hawary ME. Novel power quality indices based on wavelet packet transform for non-stationary sinusoidal and non-sinusoidal disturbances. Electr Pow Syst Res 2010; 80: 753–759.

[8] Hernandez A, Mayordomo JG, Asensi R, Beites LF. A method based on interharmonics for flicker propagation applied to arc furnaces. IEEE T Power Deliver 2005; 20: 2334–2342.

[9] Eghtedarpour N, Farjah E, Khayatian A. Intelligent identification of flicker source in distribution systems. IET Gener Transm Dis 2010; 4: 1016–1027.

[10] Altıntaş E, Salor Ö, Çadırcı I, Ermiş M. A new flicker contribution tracing method based on individual reactive current components of multiple EAFs at PCC. IEEE T Ind Appl 2010; 46: 1746–1754.

[11] Mazadi M, Hosseinian SH, Rosehart W. Instantaneous voltage estimation for assessment and monitoring of flicker indices in power system. IEEE T Power Deliver 2007; 22: 1841–1846.

[12] Perera D, Meegahapola L, Perera S, Ciufo P. Characterization of flicker emission and propagation in distribution networks with bi-directional power flows. Renew Energ 2014; 63: 172–180.

[13] Marcus IU, Nestor AE, Clarkson P. The influence of the network impedance on the nonsinusoidal (harmonic) network current and flicker measurements. IEEE T Instrum Meas 2011; 60: 2202–2210.

[14] Hsieh GC, Hung JC. Phase-locked loop techniques-A survey. IEEE T Ind Electron 1996; 43: 609–615.

[15] Karimi-Ghartemani M, Iravani MR. Robust and frequency-adaptive measurement of peak value. IEEE T Power Deliver 2004; 19: 481–489.

Appendix

Table A1. The power system bus data.

Bus	GEN (p.u.) (S = 100 MW)	Voltage (p.u.)	P load (p.u.)	Q load (p.u.)
1	0.00	1.050	0.00	0.00
2	0.50	1.050	0.00	0.00
3	0.60	1.070	0.00	0.00
4	0.00	1.000	0.70	0.70
5	0.00	1.000	0.70	0.70
6	0.00	1.000	0.70	0.70

Table A2. The power system line data.

Line no.	From	To	R (p.u.)	X (p.u.)	BCAP (p.u.)
1	1	2	0.1000	0.2000	0.0200
2	1	4	0.0500	0.2000	0.0200
3	1	5	0.0800	0.3000	0.0300
4	2	3	0.0500	0.2500	0.0300
5	2	4	0.0500	0.1000	0.0100
6	2	5	0.1000	0.3000	0.0200
7	2	6	0.0700	0.2000	0.0250
8	3	5	0.1200	0.2600	0.0250
9	3	6	0.0200	0.1000	0.0100
10	4	5	0.2000	0.4000	0.0400
11	5	6	0.1000	0.3000	0.0300